

UCRL--96913

DE87 012240

ELECTRONIC EXCITATION AND
ION SOURCE OPTIMIZATION

J. R. Hiskes
A. F. Lietzke

This paper was prepared for submittal to the
IAEA Technical Committee Meeting on Negative
Ion Beam Sources, Culham Laboratory, U.K.,
July 15-17, 1987.

June 29, 1987

The logo for Lawrence Livermore Laboratory, featuring a stylized 'U' symbol above the text 'Lawrence Livermore Laboratory' which is oriented diagonally.

Lawrence
Livermore
Laboratory

This is a preprint of a paper intended for publication in a journal or proceedings. Since changes may be made before publication, this preprint is made available with the understanding that it will not be cited or reproduced without the permission of the author.

DISCLAIMER

This document was prepared as an account of work sponsored by an agency of the United States Government. Neither the United States Government nor the University of California nor any of their employees, makes any warranty, express or implied, or assumes any legal liability or responsibility for the accuracy, completeness, or usefulness of any information, apparatus, product, or process disclosed, or represents that its use would not infringe privately owned rights. Reference herein to any specific commercial products, process, or service by trade name, trademark, manufacturer, or otherwise, does not necessarily constitute or imply its endorsement, recommendation, or favoring by the United States Government or the University of California. The views and opinions of authors expressed herein do not necessarily state or reflect those of the United States Government thereof, and shall not be used for advertising or product endorsement purposes.

ELECTRONIC EXCITATION AND ION SOURCE OPTIMIZATION

J. R. Hiskes
Lawrence Livermore National Laboratory, University of California
Livermore, CA 94550

and

A. F. Lietzke
Lawrence Berkeley Laboratory
Berkeley, CA 94720

ABSTRACT


The electronic excitation cross sections leading to $H_2(v'')$ molecules are discussed. The effect of shortening the length of the first chamber of a tandem configuration for the purpose of reducing the atomic concentration is shown to enhance the extracted current density.

Since the Grenoble Meeting in 1985 the analysis of the negative-ion hydrogen discharge has been directed both toward identifying those system parameters necessary for optimum negative ion extraction and toward clarifying the atomic density component of operating discharges.¹ At Livermore and Berkeley these efforts have been centered on the tandem system shown schematically in Fig. 1. Three principal sources of vibrational excitation are illustrated in this schematic. The excitation by fast electrons is believed to be the dominant mechanism in the high density region and this process is the focus of our discussion.

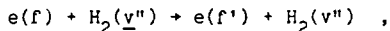
In Fig. 2 is shown the vibrational population distribution for increasing values of the first chamber electron density, n . At low densities,

*This work was performed under the auspices of the U.S. Department of Energy by the Lawrence Livermore National Laboratory under contract No. W-7405-ENG-48.

MASTER


DISTRIBUTION OF THIS DOCUMENT IS UNLIMITED

$n \ll 10^{11}$ el. cm^{-3} , the populations of the individual levels in the active portion of the spectrum are only a small fraction of a percent but are increasing with increasing density. As the electron density increases above 10^{11} toward 10^{13} - 10^{14} el. cm^{-3} however, an asymptotic distribution is achieved.² At these higher densities the populations of the excited levels become sufficiently large that their subsequent electron collisional excitation can contribute to the overall E-V process. A schematic of this process is illustrated in Fig. 3 for the $v'' = 10$ level. The calculation of cross sections for this excitation process



is summarized in Fig. 4.

For initial levels $\underline{v''} > 0$ the effective excitation cross sections are found to be enhanced over that of the ground state, $\underline{v''} = 0$. These are shown in Fig. 5 for the special case $v'' = \underline{v''}$. The effect on the vibrational population enhancement for the conditions of Fig. 2 are illustrated in Fig. 6 and expressed as a percentage enhancement, δ , for each level v'' . At this relatively low gas density, $N_2 = 10^{14}$ mol. cm^{-3} , the $v'' = 10$ enhancement approaches $\delta = 20\%$ for the asymptotic density $n = 10^{13}$ - 10^{14} el. cm^{-3} . Taking the $v'' = 10$ level as a representative case, the population enhancement is shown as a function of gas density and atom density in the next figure, Fig. 7. At higher gas and atom densities higher electron densities are required to approach the asymptote. The percentage enhancement, Δ , of the negative ion current density vs molecular density is shown in Fig. 8.

The two principal sources of atom production by electron collisions are illustrated in Fig. 9. Generation via the repulsive $^3\Sigma_u$ state leads to atoms with mean energies near 5 eV. About 20-30% of the initial excitation of the B $^1\Sigma_u$ state decays to the continuum of the X state. The resulting atomic flux from this latter dissociation channel has quite low energy, near 0.2 eV. The smaller velocity of these colder atoms increases their concentration, and their density becomes an important fraction of the total atomic density.

The higher singlet states lying above the B,C states but below the H_2^+ ionization limit contribute approximately 30% to the total singlet excitation of the $H_2(v'')$ levels and hence to their collisional destruction. At low electron densities the subsequent radiative decay of these states will contribute to the ultimate $H_2(v'')$ population, but at higher densities their collisional excitation and ionization will occur prior to radiative decay. In Fig. 11 the radiative decay and collisional excitation times are compared for selected states. The radiative decay for the B,C states is sufficiently rapid to offset excitation toward the ionization limit, but for the higher states the radiative decay is less competitive and the possibility for repopulation of the $H_2(v'')$ is lost.

At Grenoble an optimum current density of approximately 60 mA cm^{-2} was calculated for the system of Fig. 1. At this time no information was available for the relative atomic concentration, and a ratio $N_1/N_2 = 10\%$ was assumed. This N_1/N_2 ratio is a critical parameter; for a smaller ratio, $N_1/N_2 = 1\%$, the current density increases threefold.² At the Brookhaven Conference this last year a system analysis for a high electron density system concluded³ that the N_1/N_2 ratio was nearer 30%. For such a large ratio the current density is considerably depleted. The situation is summarized in Fig. 12. The principal atom-attenuation reactions are shown in Fig. 13.

To gain a perspective on the problem we show in Fig. 14 a schematic of a cylindrical tandem system and indicate the mean free paths, $\lambda(v'')$ and $\lambda(H)$, for the $H_2(v'')$ and the H atoms, respectively. Both these species are generated throughout the first chamber but only those $H_2(v'')$ generated within a centimeter of the filter have mean free path long enough to contribute to the negative ion formation in the second chamber. The H atoms generated throughout the volume contribute to the depletion of the system performance.

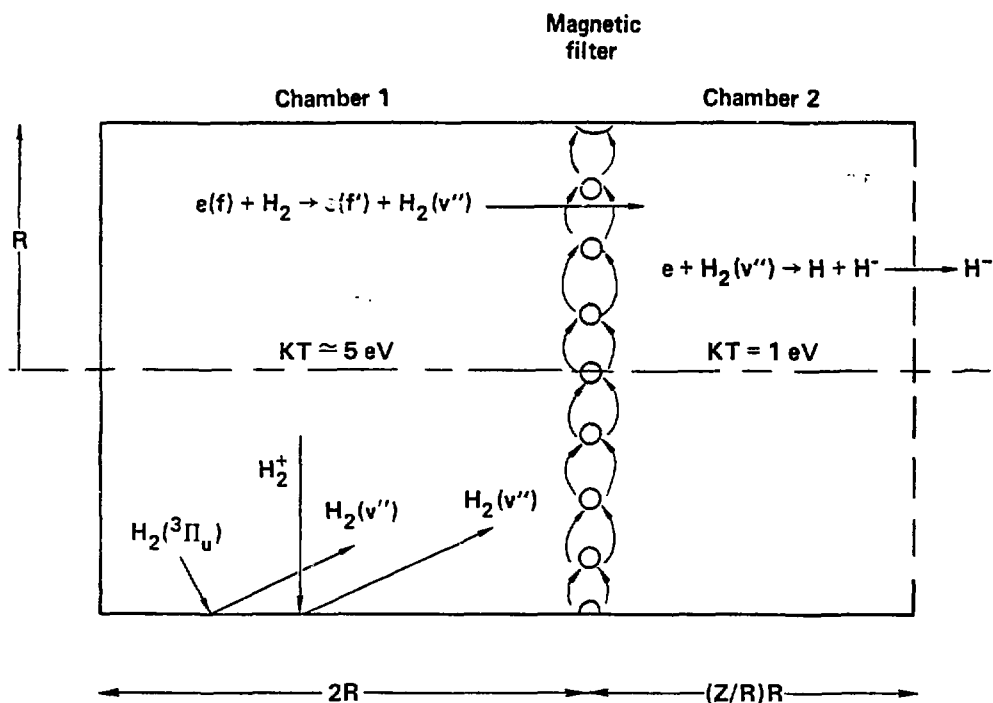
The atomic density can be reduced substantially by considering the tandem slab geometry of Fig. 15. Here the thickness, t_1 , of the first chamber slab is chosen to be comparable to the mean free path $\lambda(H_2)$. If in addition the thermal plasma of the first slab is suppressed so that the species in the first chamber consist only of $e(f)$, H_2 , H, and $H_2(v'')$, the atomic density ratio can be reduced to approximately $N_1/N_2 \approx 1\%$.

The performance of the tandem slab geometry is compared with that of the cylindrical geometry in Fig. 16. The optimum current densities available are now quite large and allow one to consider reducing the gas density below $3 \times 10^{15} \text{ mol. cm}^{-3}$. In Fig. 17 is shown the tandem-slab system performance with the gas density constrained to successively lower values but with the electron densities optimized at each gas density. The second chamber density is varied near $10^{13} \text{ el. cm}^{-3}$ to insure a maximum at one centimeter.

REFERENCES

1. AIP Conference Series, No. 158, 1987.
 2. J. R. Hiskes, A. M. Kuro, and P. A. Willmann, J. Appl. Phys. 58(5), 1759 (1985).
 3. J. R. Hiskes, A. F. Lietzke, and C. Hauck, AIP Conf. Ser., No. 158, 1987.
- PQ706026/MM

Tandem multiple-chamber system 1982



Vibrational population distribution



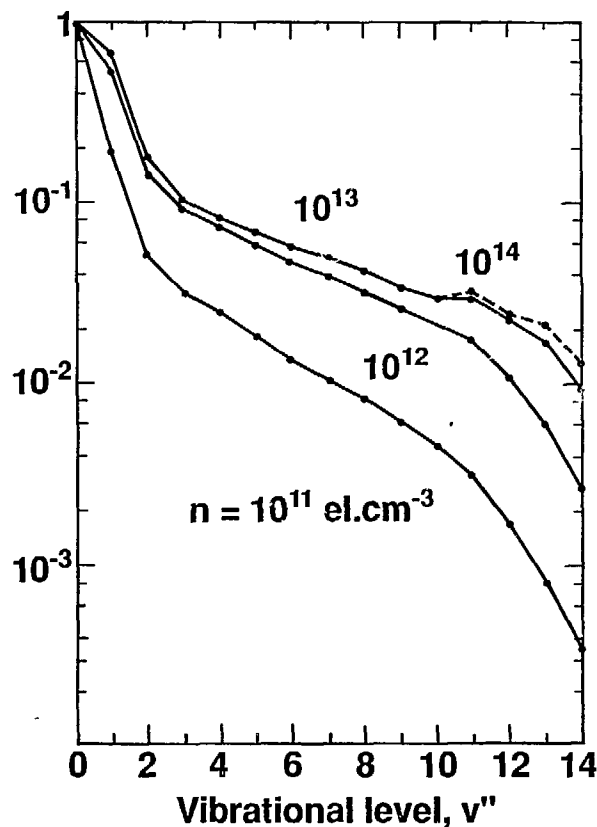
Scale length, $R = 10$ cm

$N_2 = 10^{14}$ mol. cm^{-3}

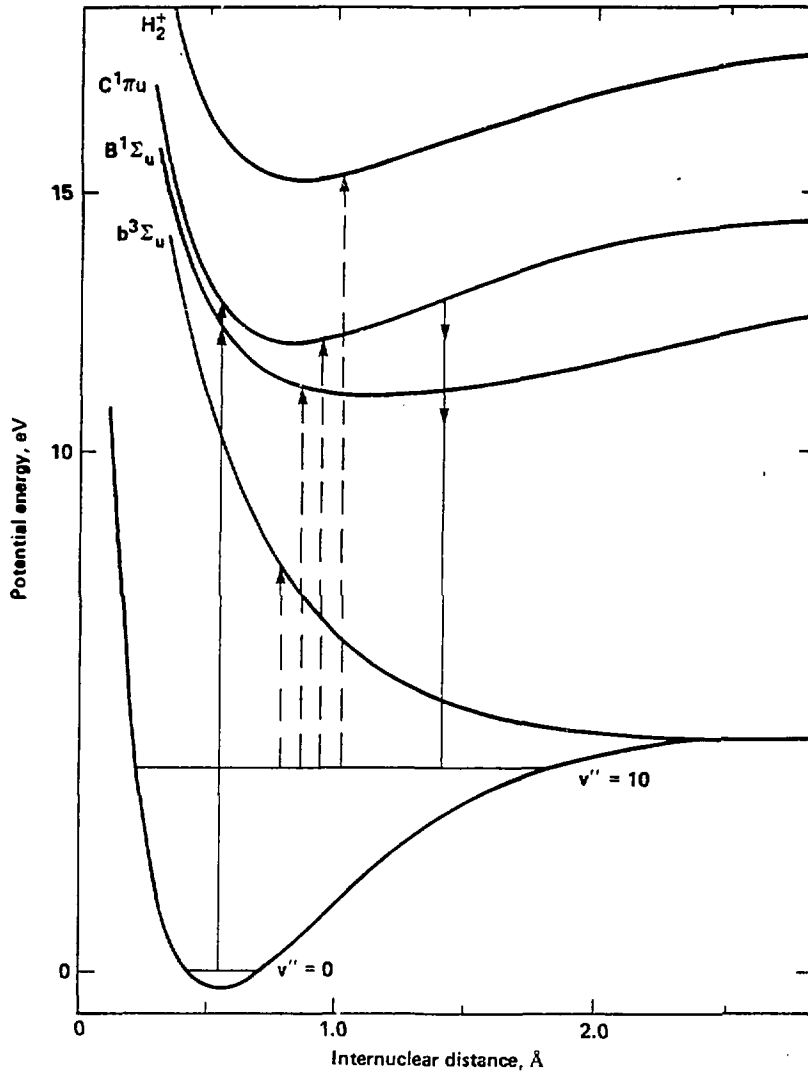
$N_1 = N_2/10$

$n(f)/n = 1/10$

Relative population, $N_2(v'')/N_2$



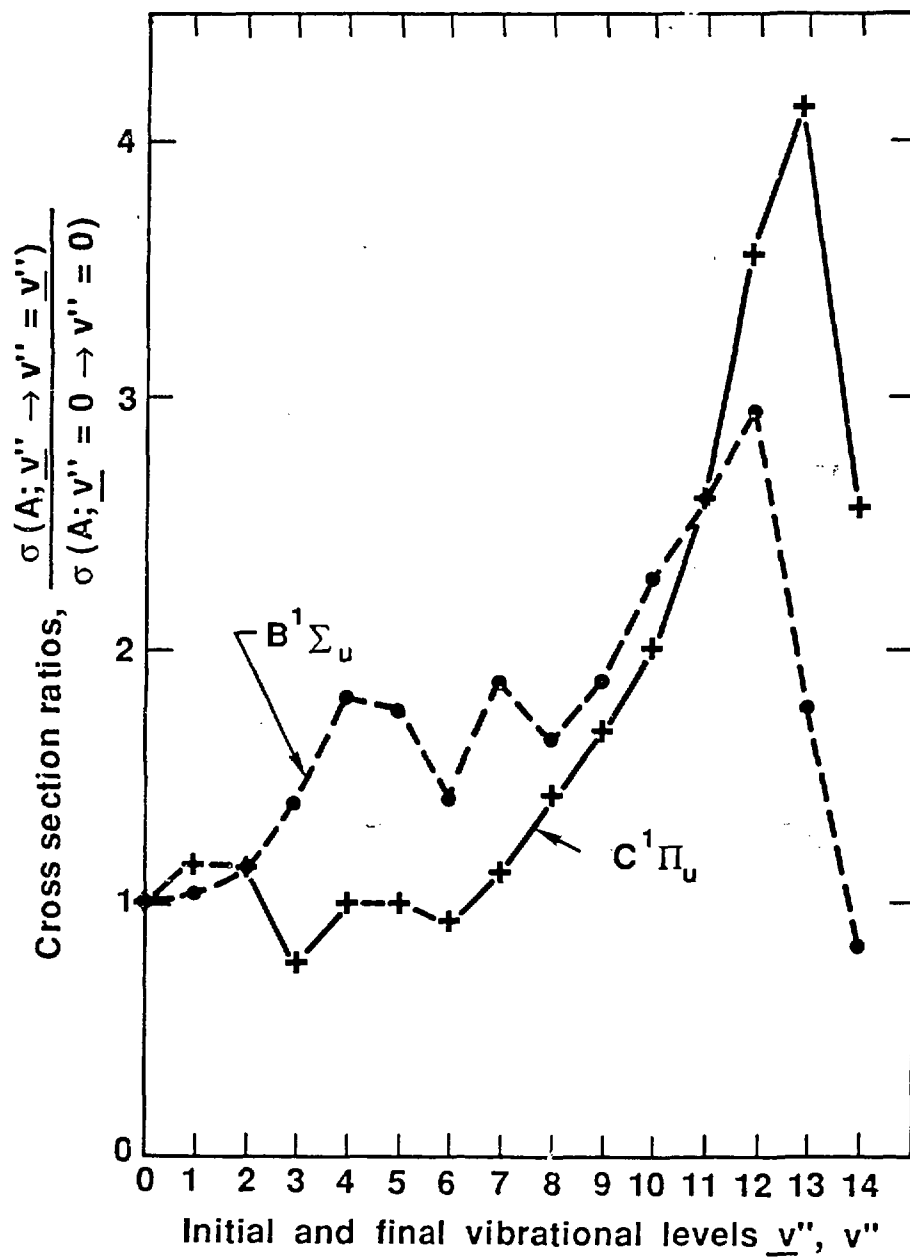
High energy electron collisional excitation of $H_2(v'')$



**Cross section for excitation of level v''
 from initial level v''
 equals
 Cross section for excitation of levels v'
 of singlet states B, C from level v''
 times
 Probability of radiative decay from v' to v''**

- **Excitation of $v' = \sigma(X-B, C) P(X, v''; B, C, v')$**
- **Probability of radiative decay from v' to v''**

$$= \frac{A(v', v'')}{\sum_{v'} [A(v'; \text{discrete } v'') + A(v'; \text{continuum } v'')]$$

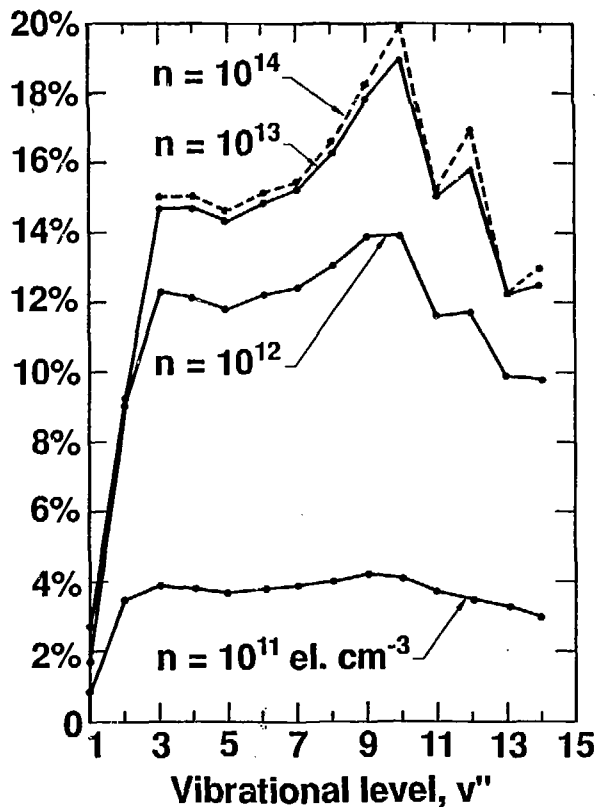


Vibrational population enhancement vs vibrational level



Scale length $R = 10 \text{ cm}$
 $10^{11} < n < 10^{14} \text{ el. cm}^{-3}$
 $N_2 = 10^{14} \text{ mol. cm}^{-3}$
 $N_1/N_2 = 1/10$

Vibrational population
enhancement, δ

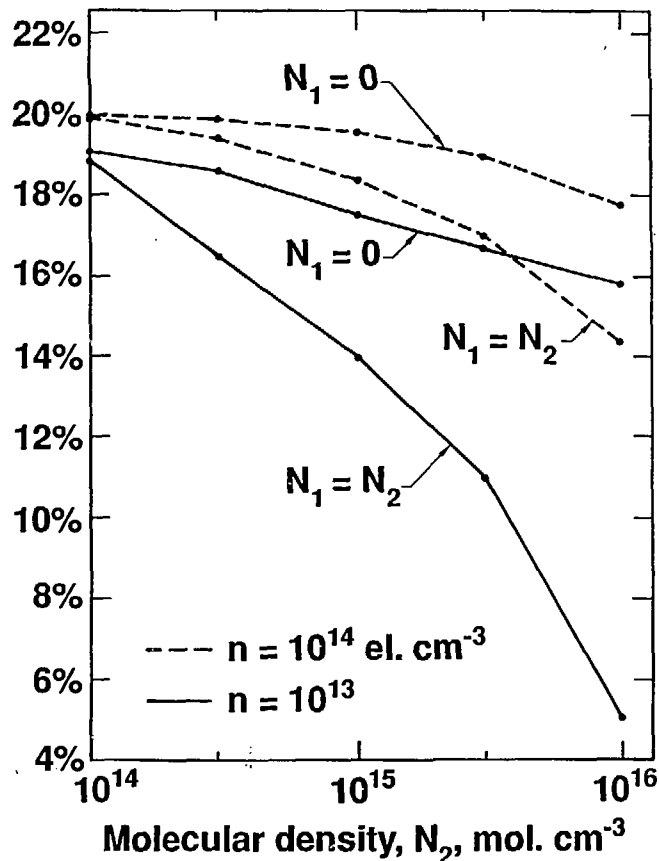


Population enhancement of the $v'' = 10$ level



Scale length, $R = 10$ cm
 $10^{13} < n < 10^{14}$ el. cm^{-3}
 $10^{14} < N_2 < 10^{16}$ mol. cm^{-3}
 $0 < N_1 < N_2$

Population enhancement
of the $v'' = 10$ level



Negative ion enhancement vs molecular density



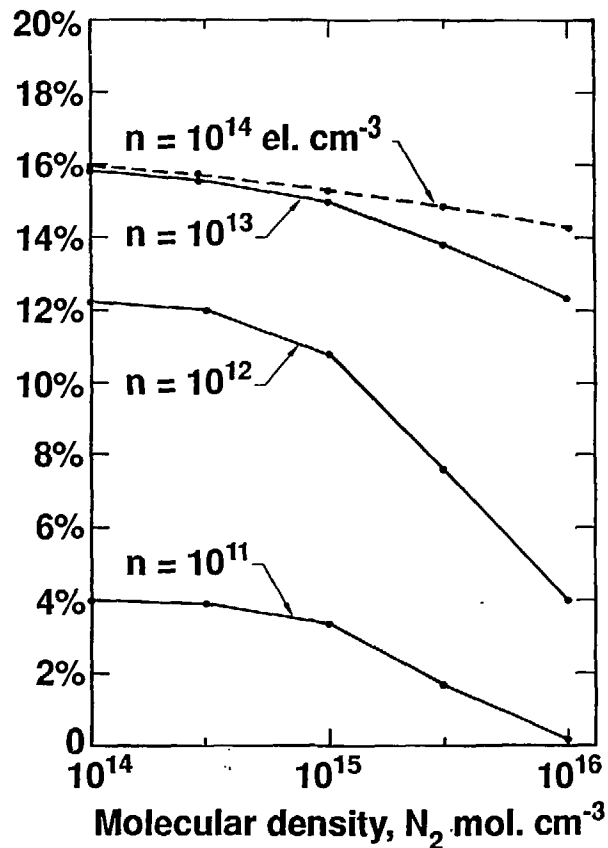
Scale length $R = 10$ cm

$10^{11} < n < 10^{14}$

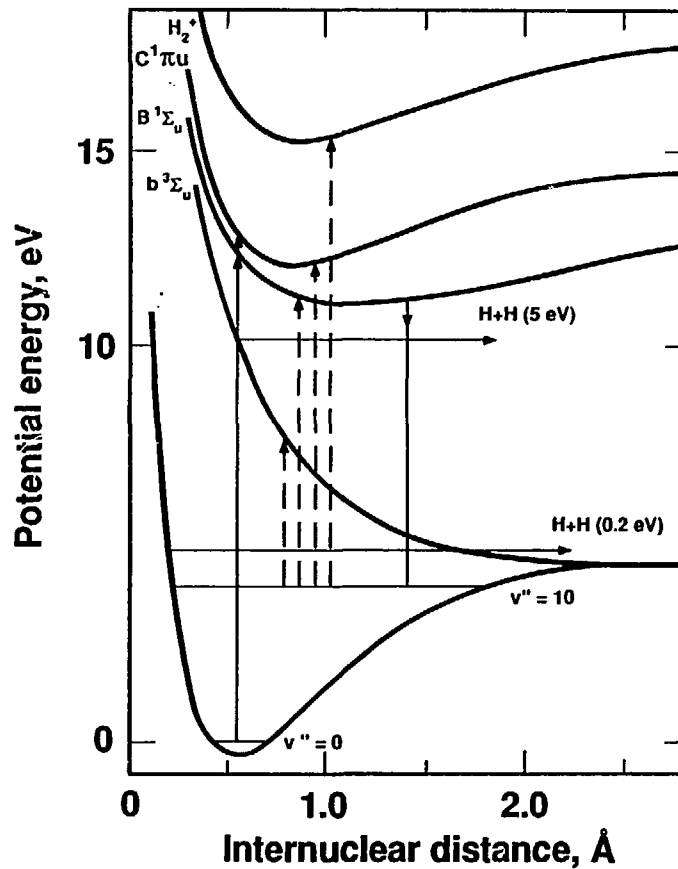
$10^{14} < N_2 < 10^{16}$

$N_1 = N_2/10$

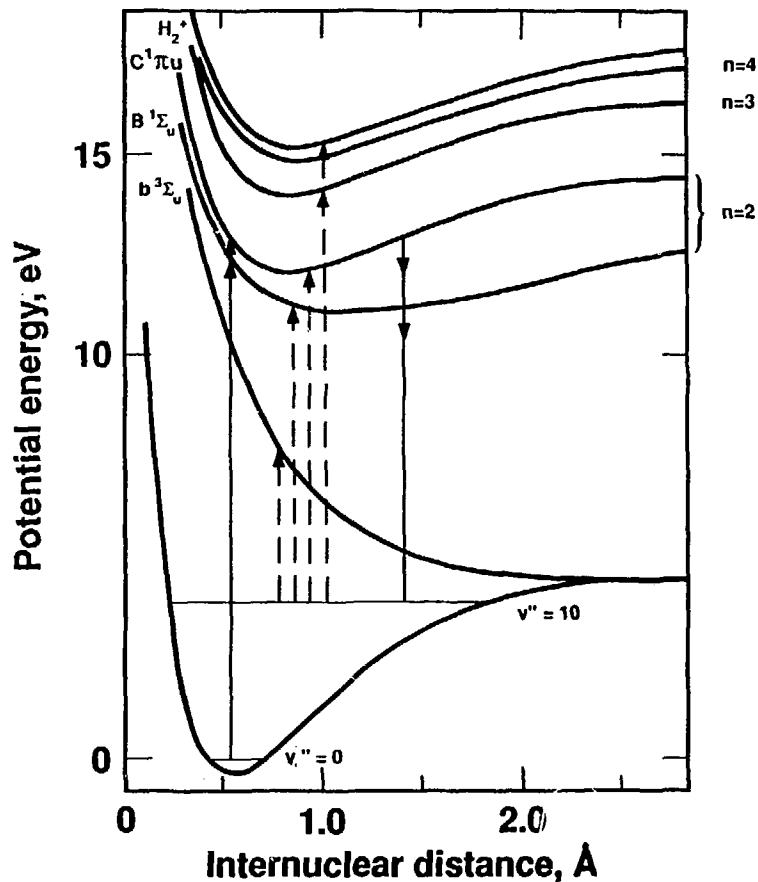
Negative ion enhancement, Δ



High energy electron collisional excitation of $H_2(v'')$



High energy electron collisional excitation of $H_2(v'')$



Comparison of collisional excitation and destruction



Radiative decay times:

$$\tau (B^1\Sigma_u, v') = 0.5 \rightarrow 1.7 \times 10^{-9} \text{ sec}$$

$$\tau (C^1\Pi_u, v') = 0.8 \rightarrow 1.0 \times 10^{-9} \text{ sec}$$

$$\tau (B''^1\Sigma_u, \dots) \cong 1 - 2 \times 10^{-8} \text{ sec}$$

Collisional excitation times:

At $n = 10^{13}$ electrons cm^{-3}

$$\tau (B^1\Sigma_u, C^1\Pi_u) = 1/n\sigma v \cong 3 \times 10^{-7} \text{ sec}$$

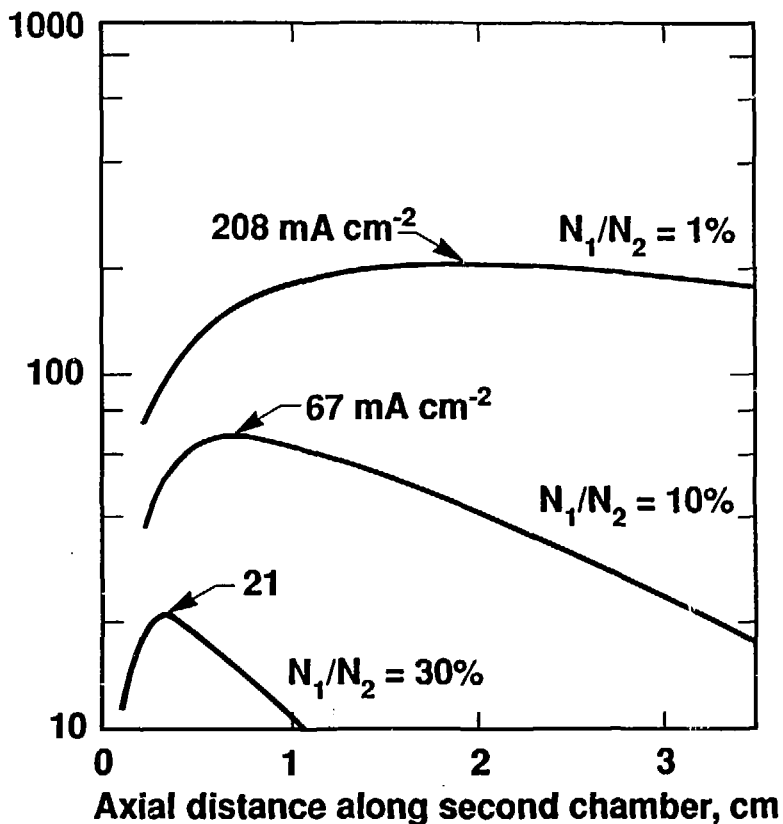
$$\tau (B''^1\Sigma_u, \dots) \cong 2 \times 10^{-8} \text{ sec}$$

Optimized tandem system, Grenoble, 1985



Scale Length, 10 cm
Hydrogen Density
 $N_2 = 3 \times 10^{15} \text{ mol. cm}^{-3}$

Negative ion current
density, mA cm^{-2}

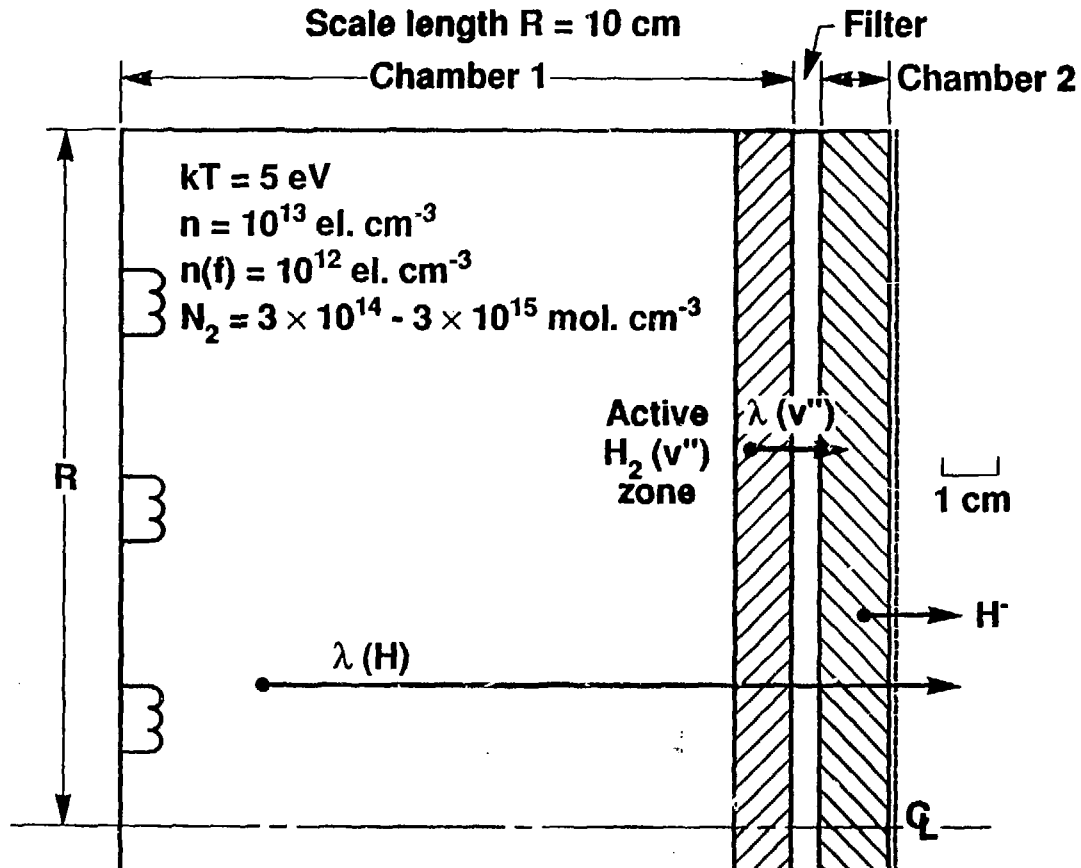


Atomic destruction processes

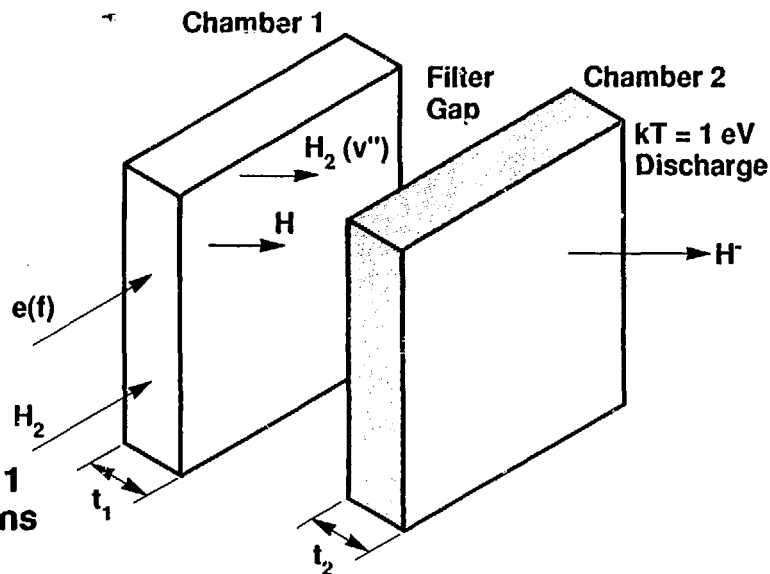


- $\text{H} + \text{H}_2 (v'') \rightarrow \text{H} + \text{H}_2 (v' < v'')$
- $\text{H} + \text{H}_2 (v'') \rightarrow \text{H} + \text{H} + \text{H}$
- $\text{H} + \text{H}^- \rightarrow \text{H}_2 (v'') + \text{e}$

Perspective of active regions of a tandem discharge



Tandem slab geometry



- No Losses in Chamber 1 Due to Thermal Electrons
- Minimal Atom Losses
- Atomic Density Ratio:

Volume Generation = Outward Flux

$$n(f) N_2 \sigma v (\text{diss.}) A t_1 = 2 A N_1 v(A)$$

$$N_1/N_2 = \frac{t_1}{2} \frac{n(f) \sigma v (\text{diss.}; {}^3\Sigma_u, {}^1\Sigma_u)}{v(A)} \cong 1\%$$

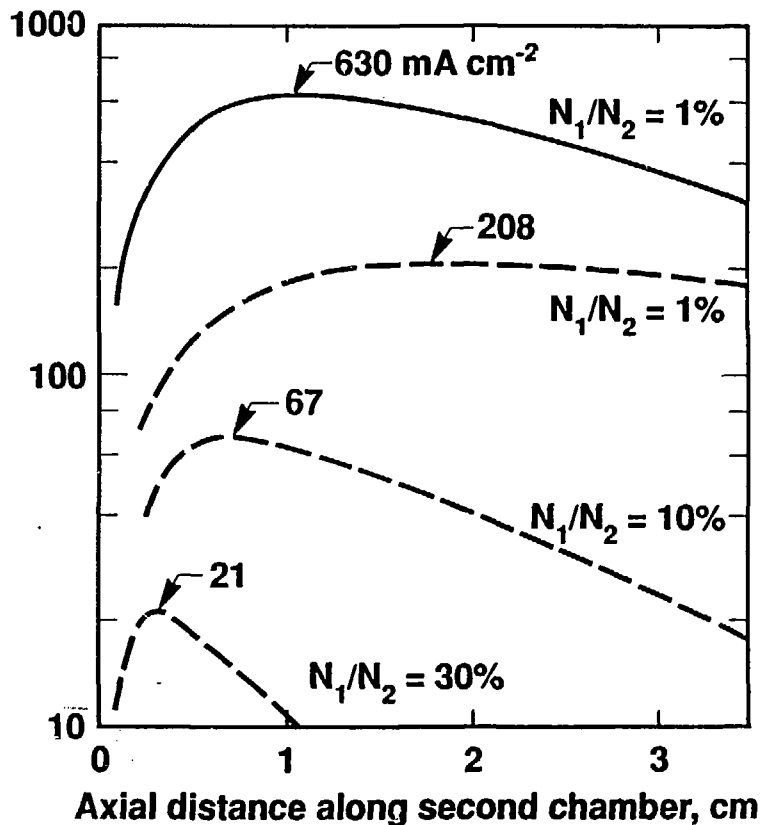
$$t_1 \leq 2 \text{ cm}, t_2 \cong 1 \text{ cm}$$

Comparison of cylindrical and tandem slab geometries



Scale length, 10 cm
 $N_2 = 3 \times 10^{15} \text{ mol. cm}^{-3}$
 $n(2) \cong 10^{13} \text{ el. cm}^{-3}$

Negative ion current
 density, mA cm^{-2}



Tandem slab geometry



Scale length, 10 cm

$N_1/N_2 = 1\%$

$n(f) = 0.8 \times 10^{12} \text{ el. cm}^{-3}$

Negative ion current
density, mA cm^{-2}

